Studies of J Dependence in Neutron Pickup Reactions*

C. GLASHAUSSER†
Princeton University, Princeton, New Jersey
AND
M. E. RICKEY‡
University of Colorado, Boulder, Colorado
(Received 1 August 1966)

The dependence of the form of angular distributions on the total angular momentum transfer (J dependence) has been studied for the following reactions: $Fe^{56}(p,d)Fe^{55}$ at 18.5, 20.0, 22.4, 25.7, and 27.5 MeV; $Ni^{58}(p,d)Ni^{57}$ at 20.0, 25.4, and 27.5 MeV; $C^{12}(p,d)C^{11}$, $S^{32}(p,d)S^{31}$, and $Pb^{208}(p,d)$ Pb^{207} at about 28 MeV and $Fe^{56}(He^3,\alpha)Fe^{55}$ at 30 and 40 MeV. Pronounced J dependence was found to persist for both $l=1$ and $l=3$ transfers in the $Fe^{56}(p,d)Fe^{55}$ and $Ni^{58}(p,d)Ni^{57}$ reactions over the entire energy range; changes with energy are gradual but definite. The spin dependence of $l=2$ distributions in the $S^{32}(p,d)S^{31}$ reaction is equally striking, but essentially no J dependence was observed for either $l=1$ or $l=3$ transfer in the $Pb^{208}(p,d)Pb^{207}$ reaction. Apparent Q dependence makes the interpretation of the $C^{12}(p,d)C^{11}$ results ambiguous. The $Fe^{56}(He^3,\alpha)Fe^{55}$ reaction revealed small but noticeable phase differences between $\frac{5}{2}^-$ and $\frac{7}{2}^-$ distributions. Analysis of the $Fe^{56}(p,d)Fe^{55}$-distributions with the distorted wave Born approximation was not successful in explaining the results. Finite-range nonlocal calculations including spin-orbit forces in both incoming and outgoing channels and/or modified neutron form factors predicted little J dependence.

I. INTRODUCTION

THERE is now impressive evidence that the angular distribution of the outgoing particles in a wide variety of direct reactions depends on the total angular momentum transfer J as well as on the orbital angular momentum transfer l. Lee and Schiffer[1] were the first to point out systematic differences in the large-angle behavior of $\frac{3}{2}^-$ and $\frac{1}{2}^-$ differential cross sections. Soon afterwards, Sherr, Rost, and Rickey[2] reported J dependent effects in the forward angles of $l=3$ (p,d) curves, and Fulmer and Daehnick[3] observed $l=1$ J dependence in the (d,t) reaction. More recently, J dependence has been found in (α,p),[4] (p,α),[5] (He^3,d),[6] (He^3,α),[7,8] and (d,n)[9] reactions.

In the (d,p) reaction, the backward angle dip characteristic of $\frac{1}{2}^-$ distributions has been observed at energies from 7–15 MeV, on targets ranging from C^{12} to Ni^{62}. (It is not seen at 6 MeV.) The $l=2$ transitions show a strong J dependence in the $2s$-$1d$ shell at incident energies around 12 MeV[10]; the differences between $\frac{3}{2}^+$ and $\frac{5}{2}^+$ distributions are less pronounced in the $2d$ shell at 12 MeV,[11] and not noticeable at 15 MeV.[12,13] The only reported $l=3$ data relevant to J dependence revealed forward and backward angle differences between $\frac{5}{2}^-$ and $\frac{7}{2}^-$ curves at 10 MeV.[14] The forward angles showed effects similar to those observed by Sherr *et al.*[2] in (p,d): The $\frac{5}{2}^-$ curves peak at a more forward angle and decrease more abruptly from this maximum than $\frac{7}{2}^-$ curves. Similar, but not so pronounced, J dependence has been found recently by Cavanagh *et al.*[15] for $l=2$ transfer in (p,d) reactions on the Sn isotopes at 30 MeV. The $\frac{1}{2}^-$ back angle dip observed in (d,p) has also been seen in (p,d) on Fe^{56} at 17.5 MeV.[16]

One great value of J dependence lies in its usefulness in determining the spins of excited states. Until the mechanism responsible for J dependence is well understood, these spins should probably not be regarded as definite. However, for empirically well explored transitions such as $l=1$ transfer in (d,p), the assignment is very probable. Ten such new assignments were made by Lee and Schiffer[1] in their original work. In addition, new $\frac{3}{2}^-$ and $\frac{1}{2}^-$ states have been determined, for example,

* Work performed under U. S. Atomic Energy Commission Contracts at University of Colorado and Princeton University.
† Present address: Service de Physique Nucleaire A Moyenne Energie, Centre d'Etudes Nucleaires, Saclay, 91-Gif sur Yvette, France.
‡ Present address: University of Indiana, Bloomington, Indiana.
[1] L. L. Lee, Jr., and J. P. Schiffer, Phys. Rev. Letters **12**, 108 (1964).
[2] R. Sherr, E. Rost, and M. E. Rickey, Phys. Rev. Letters **12**, 420 (1964).
[3] R. H. Fulmer and W. W. Daehnick, Phys. Rev. Letters **12**, 455 (1964).
[4] L. L. Lee *et al.*, Phys. Rev. Letters **14**, 261 (1965).
[5] J. A. Nolen, Jr., C. Glashausser, and M. E. Rickey, Phys. Letters **21**, 705 (1966).
[6] A. G. Blair, Phys. Rev. **140**, B648 (1965).
[7] Claus Mayer-Böricke, R. H. Siemssen, and L. L. Lee, Jr., Bull. Am. Phys. Soc. **10**, 26 (1965).
[8] M. K. Brussel, D. E. Rundquist, and A. I. Yavin, Phys. Rev. **140**, B838 (1965).
[9] S. G. Buccino, D. S. Gemmell, L. L. Lee, Jr., J. P. Schiffer, and A. B. Smith, Bull. Am. Phys. Soc. **10**, 511 (1965).
[10] J. P. Schiffer, L. L. Lee, Jr., A. Marinov, and C. Mayer-Böricke, Bull. Am. Phys. Soc. **10**, 510 (1965).
[11] L. L. Lee, Jr., A. Marinov, Claus Mayer-Böricke, and J. P. Schiffer, Bull. Am. Phys. Soc. **9**, 651 (1964).
[12] R. Sass, B. Rosner, and E. Schneid, Phys. Rev. **138**, B399 (1965).
[13] E. K. Lin, Phys. Rev. **139**, B340 (1965).
[14] J. L. Alty, L. L. Green, G. D. Jones, and J. F. Sharpey-Schafer, Phys. Letters **13**, 55 (1964).
[15] P. E. Cavanagh, C. F. Coleman, J. F. Turner, A. G. Hardacre, G. A. Gard, and D. A. Boyce, Rutherford Laboratory Progress Report, 1965 (unpublished).
[16] Charles A. Whitten, Jr., E. Kashy, and J. P. Schiffer, Bull. Am. Phys. Soc. **9**, 650 (1964).

in A^{37},[17] Ca^{41},[18] Ca^{47},[19] and Ca^{49},[20] as well as $\frac{3}{2}^+$ states in Si^{29},[10] S^{33},[10] and Ca^{41}.[18] Sherr *et al.*[2] found J dependence useful also in fixing the spins of several levels in their (p,d) work. In other reactions, especially those involving He^3 projectiles, the spin assignments must be regarded more tentatively, since the J dependence has not yet been thoroughly studied.

Even when new spin assignments are not made, however, the very occurrence of J dependence is a potentially rich source of information about the reaction mechanism. The standard theoretical treatments of direct reactions scarcely mention the possibility that the shape of the differential cross section might depend on J. Certainly the very pronounced differences were in no sense predicted beforehand by the theory. But now that a strong J dependence has been well verified experimentally, it is interesting to find out whether the standard distorted-wave Born approximation (DWBA) can fit the data when spin-orbit terms are included in the potentials, and corrections are made for finite range and nonlocality.

In an attempt to answer such questions about the reaction mechanism, and to provide a systematic basis for DWBA calculations, a number of experiments were carried out at the University of Colorado cyclotron. The $Fe^{56}(p,d)Fe^{55}$ reaction was selected for intensive study, since reasonably well separated levels of known spin in Fe^{55} can be reached by $l=1$ and $l=3$ transfers, with both $J=l+\frac{1}{2}$ and $J=l-\frac{1}{2}$. The angular distribution of deuterons from 17.5°–145° was measured at five energies, 18.5, 20.0, 22.4, 25.7, and 27.5 MeV, in order to determine whether any systematic changes in the $l=1$ or $l=3$ J dependence occurred in this energy interval. Such changes might be expected in the $\frac{1}{2}^-$ curve, for example, if an interference sensitive to the momentum of either particle is responsible for the deep minima observed. If small changes in the radial wave function of the neutron inside the nucleus corresponding to $j=\frac{5}{2}$ and $\frac{7}{2}$ cause the differences between two $l=3$ curves, this J dependence might disappear at lower energies when the reaction tends to take place further from the center of the nucleus. A spin-orbit potential concentrated at the nuclear surface would also be expected to have different effects on the angular distribution at different energies for this reason. In addition, the optical model parameters used in the DWBA analyses of the (p,d) distributions can be chosen so that they fit elastic scattering data over a large energy region, and thus do not reflect peculiarities of one particular measurement or fit to the data. This is important in deciding whether the DWBA gives a reasonably consistent account of J dependence.

The $Ni^{58}(p,d)Ni^{57}$ reaction was studied in less detail at three energies, 20.0, 25.4, and 27.5 MeV, in order to confirm the Fe^{56} data. Any effects that are strongly dependent on the detailed structure of the nuclear states should be reflected in differences in the angular distributions for states of the same J in Fe^{55} and Ni^{57}.

In an effort to see whether J dependence is still present in other regions of the periodic table, angular distributions for the reactions $C^{12}(p,d)C^{11}$, $S^{32}(p,d)S^{31}$, and $Pb^{208}(p,d)Pb^{207}$ were also measured, at an energy of about 28 MeV. These measurements of distributions leading to the 1.24-MeV $\frac{3}{2}^+$ and 2.23-MeV $\frac{5}{2}^+$ states in S^{31} can be compared with the results of Kavaloski *et al.*[21] at 40 MeV which show little, if any, J dependence. With the measurement of $l=1$ distributions for $\frac{3}{2}^-$ and $\frac{1}{2}^-$ states in C^{11} and Pb^{207}, holes in the $1p$ and $3p$ shells are studied. The $2p$ and $1f$ shells are investigated in Fe^{56}, and the Pb^{208} data involve the $2f$ shell also. The different numbers of nodes in the radial wave functions of the neutrons might play some role in determining whether the distributions will be J-dependent. However, the different sizes, volume-to-surface ratios, Coulomb barriers, optical potentials, and structures of the states are probably equally important in their effect on the angular distributions. It is interesting to see whether J dependence persists in spite of these changes.

Finally, the $Fe^{56}(He^3,\alpha)Fe^{55}$ reaction, which involves two very strongly absorbed particles, was investigated at 30 and 40 MeV. The J dependence reported in this reaction at 17.5 MeV by the Argonne group[7] was not very pronounced. An increase in the bombarding energy reduces the Coulomb distortion and allows the incoming particle to penetrate further into the nucleus; thus we might expect to see significant changes in the J dependence at the higher energy.

The results of these experiments are discussed in

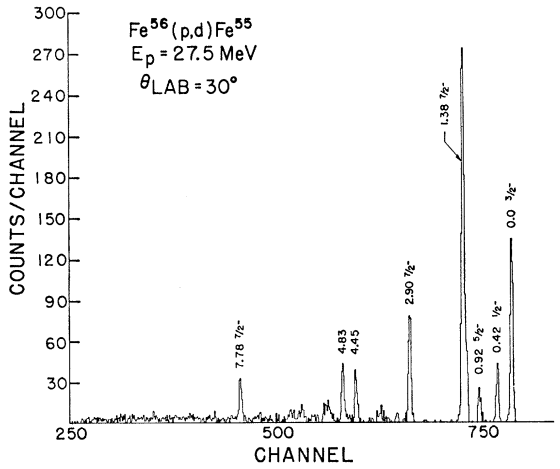

FIG. 1. A spectrum of deuterons at 30° from the $Fe^{56}(p,d)Fe^{55}$ reaction at 27.5 MeV. Excitation energies and known spins are marked for strong peaks.

[17] Baruch Rosner and Edward J. Scheid, Phys. Rev. **139**, B66 (1965).
[18] T. A. Belote, A. Sperduto, and W. W. Buechner, Phys. Rev. **139**, B80 (1965).
[19] J. H. Bjerregaard, Ole Hansen, and G. Sidenius, Phys. Rev. **138**, B1097 (1965).
[20] E. Kashy, A. Sperduto, H. A. Enge, and W. W. Buechner, Phys. Rev. **135**, B865 (1964).
[21] C. D. Kavaloski, G. Bassani, and Norton M. Hintz, Phys. Rev. **132**, 813 (1963).

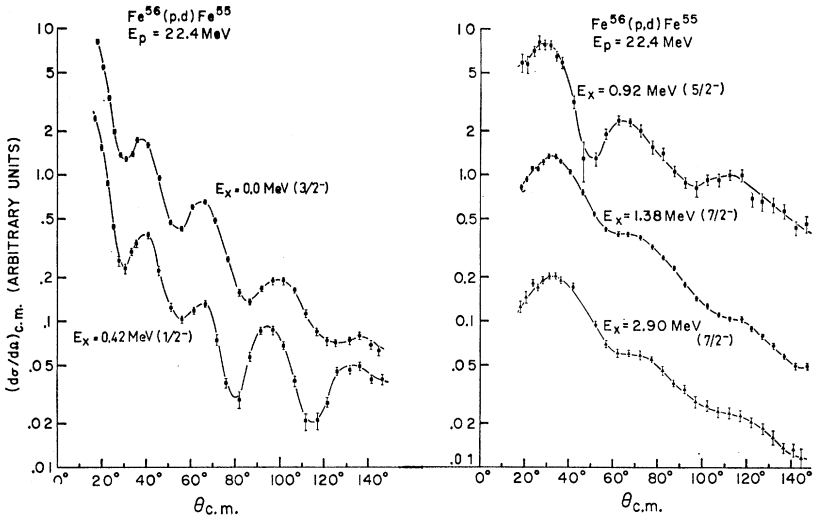

FIG. 2. Angular distributions of deuterons from the $Fe^{56}(p,d)Fe^{55}$ reaction at 22.4 MeV, with arbitrary normalization. The errors shown include contributions from poor peak separation when necessary. The lines are visual guides.

Sec. III, after a brief description of the experimental techniques in Sec. II. Recent attempts at fitting J dependence are reviewed in Sec. IV, followed by a comparison of the present $Fe^{56}(p,d)Fe^{55}$ data with DWBA predictions. Section V summarizes the results obtained.

II. EXPERIMENTAL PROCEDURE

The experiments were carried out at the University of Colorado AVF cyclotron. The particle identification system and beam optics have been described previously.[22] Beam currents on the target ranged up to 400 nA for protons, and 200 nA for He^3. Over-all energy resolution was as good as 70 keV for protons and 100 keV for He^3. The He^3 was continuously recovered, purified, and recirculated in a trapping system which is a modified version of the one described by Wegner and Hall.[23] The integrated current from a Faraday cup and a scintillation-counter monitor were used to compute cross sections.

Outgoing particles were detected in a three-counter telescope of Ortec surface barrier detectors, generally 300-, 2300 , and 300-μ thick, respectively. The over-all angular resolution was about 2.5° full width. A very stable and linear pulse multiplier[24] employing field-effect transitors allowed easy particle identification. Spectra were taken in one dimension of an ND-160 analyzer, gated by a coincidence between pulses from the ΔE and E–ΔE detectors and the output of the differential discriminator selecting the desired particle. An anticoincidence pulse from the third detector rejected high-energy protons.

The energy of the proton beam was determined by measuring the crossover angle[25] for protons scattered from H and the C^{12} 4.4- or 9.6-MeV states, using a CH target. Measuring this angle to ±0.15° on both sides of the beam gives the energy to about ±150 keV and fixes the zero angle. The correction to the nominal zero was less than ±0.5°.

III. EXPERIMENTAL RESULTS

A. $Fe^{56}(p,d)Fe^{55}$

The $Fe^{56}(p,d)Fe^{55}$ reaction was studied at five energies, 18.5, 20.0, 22.4, 25.7, and 27.5 MeV. Figure 1 shows an energy spectrum of deuterons from a 27.5-MeV run at 30°, together with previously proposed spin assignments. The energies of the excited levels are those measured by Sherr *et al.*[22]

The ground-state spin is $\frac{3}{2}^-$. The spin of the 0.42-MeV state is now well-established as $\frac{1}{2}^-$ on the basis of an $(n,\gamma\gamma)$ angular correlation measurement.[26] The 0.92-MeV state is known to be $\frac{5}{2}^-$, and one at 1.413 MeV is $\frac{7}{2}^-$.[27] The state marked 1.38 MeV in Fig. 1 is a doublet, consisting of the 1.413-MeV state and another, less strongly excited state at 1.327 MeV. The spin of the latter state is not certain, but it shows an $l=3$ stripping pattern, and a comparison of (d,p)[28] and (p,d)[22] cross sections indicates it is $\frac{7}{2}^-$. Whitten[29] was able to resolve the 1.327 from the 1.413 level in (p,d) measurements at 17.5 MeV; he found that the ratio of the cross sections for the two states is about 1:4. If the spin of the weaker state is actually $\frac{5}{2}^-$, then it would, of course, tend only

[22] R. Sherr, B. Bayman, E. Rost, M. E. Rickey, and C. G. Hoot, Phys. Rev. **139**, B1272 (1965).
[23] H. E. Wegner and W. E. Hall, Rev. Sci. Instr. **29**, 1100 (1958).
[24] G. L. Miller and V. Radeka, Brookhaven National Laboratory Report No. BNL-6952 (unpublished); V. Radeka, IEEE trans. Nucl. Sci., **NS-11**, 358 (1964).
[25] B. M. Bardin and M. E. Rickey, Rev. Sci. Instr. **35**, 902 (1964); Rodman Smythe, *ibid.* **35**, 1197 (1964). The technique was also described by F. H. Schmidt *et al.*, Nucl. Phys. **52**, 363 (1964).
[26] R. E. Coté, H. E. Jackson, Jr., L. L. Lee, Jr., and J. P. Schiffer, Phys. Rev. **135**, B52 (1964).
[27] R. W. Bauer and M. Deutsch, Nucl. Phys. **16**, 264 (1960).
[28] R. H. Fulmer and A. L. McCarthy, Phys. Rev. **131**, 2133 (1963).
[29] Charles A. Whitten, Jr., thesis, Princeton University, 1966 (unpublished).

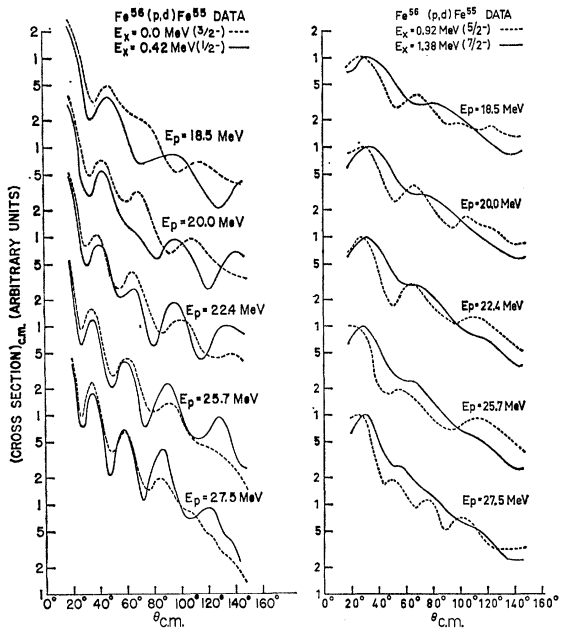

FIG. 3. Energy dependence of angular distributions of deuterons from the $Fe^{56}(p,d)Fe^{55}$ reaction. Curves for $l=1$ are shown on the left, and for $l=3$ on the right. The error bars of Fig. 2 are typical of all these data.

to wash out slightly any differences between the 1.38- and the 0.92-MeV differential cross sections. The state at 2.90 MeV is assigned spin $\frac{7}{2}^-$ since it is seen strongly in (p,d) and not at all in (d,p).

Center-of-mass angular distributions for the 22.4-MeV run are shown in Fig. 2. Data were taken every 2.5°, from 17.5° to 40°, and every 5° thereafter to 145°. The number of data points and the error bars shown here are typical of the Fe^{56} results at all energies. The errors shown are mainly statistical, but when there was some difficulty in separating two peaks, a reasonable error was assigned and included in the error bars shown. Background counts were always negligible. The lines are merely drawn through the points, and the scales are arbitrary. Figure 3 shows the energy dependence of the $l=1$ and $l=3$ distributions. Finally, the ratio of the ground-state cross section to the 0 42-MeV state cross section at the five energies is shown in Fig. 4, and a similar plot of the 0.92 MeV/1.38 MeV cross-section ratio is illustrated in Fig. 5. Such plots, first used by Fulmer and Daehnick,[3] show the J dependence strikingly.

The dependence of the angular distributions on J as well as l can be clearly seen from these figures. The $l=1$ J dependence is quite pronounced at all energies studied, but the differences are most noticeable at 18.5 and 20 MeV. At these energies the two distributions have quite different shapes, especially at angles greater than 50°. In the 18.5-MeV curve, the $\frac{1}{2}^-$ drops sharply to a minimum at 70° and is relatively smooth out to 100°, where it again begins to decrease rapidly to a minimum at 130°. The latter corresponds to the back angle minimum seen in the (d,p) work of Lee *et al.*[1] However, the J dependence around 70° is just as definite as the back-angle differences, since the $\frac{3}{2}^-$ curve has an incipient maximum at 70° and a minimum at 90°. (This behavior is well reproduced in the $l=1$ data of Whitten[29] for $Cr^{54}(p,d)Cr^{53}$ at 17.5 MeV.) At 20 MeV, the $\frac{3}{2}$ shows a definite maximum at 70°, and the $\frac{1}{2}$ is beginning to fill in the valley seen at 18.5 MeV. These large differences are reflected in the height of the ratio peaks at 70° in Fig. 4 at 18.5 and 20 MeV. At higher energies, the ratio peaks become less prominent as the differences between the $\frac{3}{2}$ and $\frac{1}{2}$ patterns become differences in over-all structure rather than in shape. At these energies, the $\frac{1}{2}$ curve oscillates more sharply than the $\frac{3}{2}$, and does not decrease as quickly at the very large angles. It is important to note that there is only slight evidence for a phase shift between the two curves at the higher energies; the maxima and minima tend to occur at the same angle for each distribution.

The forward-angle J dependence in the $l=3$ curves is just about the same at all five energies. These data are consistent with the forward-angle measurements at 28 MeV, of Sherr *et al.*,[2] who first noticed the shift of the $\frac{5}{2}^-$ curve relative to the $\frac{7}{2}^-$. This shift is less well defined at the lower energies, since the actual peak position becomes more difficult to determine as the

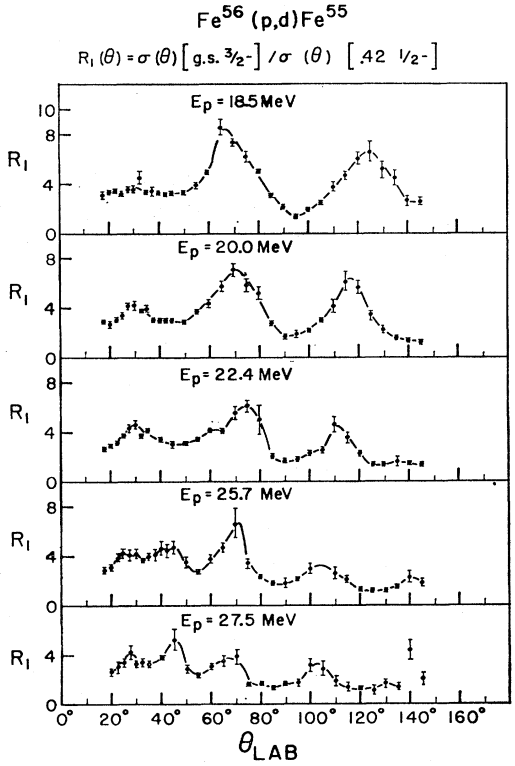

FIG. 4. The ratio of the (p,d) cross section for the ground state $(\frac{3}{2}^-)$ of Fe^{55} to the cross section for the 0.42-MeV $(\frac{1}{2}^-)$ state in the same final nucleus.

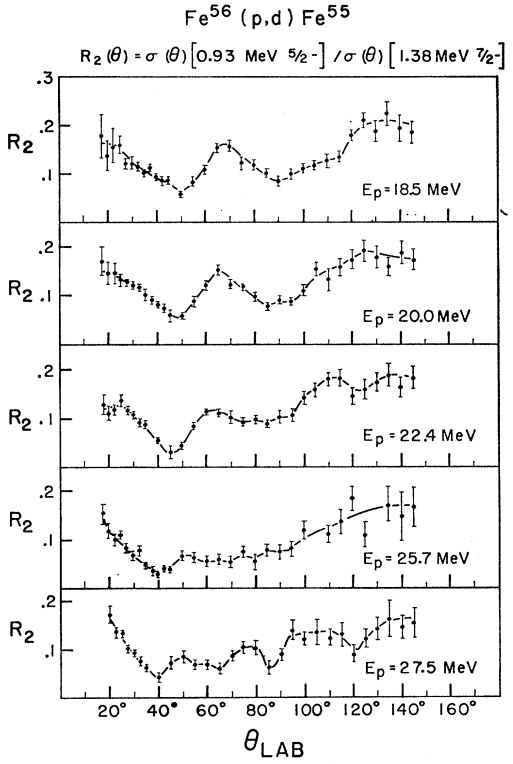

FIG. 5. The ratio of the (p,d) cross section for the 0.93-MeV ($\frac{5}{2}^-$) state in Fe^{55} to the cross section for the 1.38-MeV ($\frac{7}{2}^-$) state in the same final nucleus.

peaks get broader. However, the two curves are always between 5° and 10° apart at the half-maximum point. At larger angles, the $\frac{7}{2}$ cross section assumes a gently varying shape, while the $\frac{5}{2}$ distribution reveals a very definite second maximum at the lower energies and a general increase in structure at 27.5 MeV. Like the $\frac{1}{2}$ relative to the $\frac{3}{2}$, the $\frac{5}{2}$ also falls off less rapidly than the $\frac{7}{2}$ at the backward angles.

B. $Ni^{58}(p,d)Ni^{57}$

The (p,d) reaction on Ni^{58} was investigated at 20.0, 25.4, and 27.5 MeV to corroborate the results of the Fe^{56} study. Angular distributions were measured for states at 0.0, 0.78, 1.12, 2.59, and 5.22 MeV. The ground state has spin $\frac{3}{2}^-$; recent (d,t)[30] and (He^3,α)[8] results indicate that the 1.12-MeV level is a $\frac{1}{2}^-$ state. The 0.78-MeV level was assigned $\frac{5}{2}^-$, and the 2.59- and 5.22-MeV states $\frac{7}{2}^-$ by Sherr *et al.*[22] on the basis of forward angle J dependence. (The 5.22-MeV state is the isobaric analog state.)

The Ni^{58} data are not as complete as the Fe^{56} data shown above; the points are fewer and the error bars larger, especially for the $\frac{1}{2}^-$ (1.12 MeV) state whose cross section is now a factor of ten smaller than the ground-state cross section. Typical distributions are shown in Fig. 6. The lines on these plots are the experimental curves for the $Fe^{56}(p,d)Fe^{55}$ reaction at the same energy.

The main features of the Fe^{56} distributions are very well reproduced by the Ni^{58} data. Except at 20 MeV, the $l=1$ angular distributions for Fe^{56} and Ni^{58} just about overlap within the errors. The $l=1$ Ni^{58} angular distributions at 20 MeV look more similar to the Fe^{56} data at 18.5 MeV than at 20 MeV, which is an indication that Q-value effects are important at the lower energy. (The ground state Q is -9.0 MeV for Fe^{56} and -10.0 MeV for Ni^{58}.) Even so, the ratio curves for Fe and Ni are remarkably similar at 20 MeV as well as at the higher energies. The Q value has some effect also on $l=3$ transitions; Ni^{58} distributions are generally shifted to slightly larger angles relative to the Fe^{56} data. Again, though, the J dependence is definitely present, and closely matches the J dependence observed in Fe^{56} at all energies.

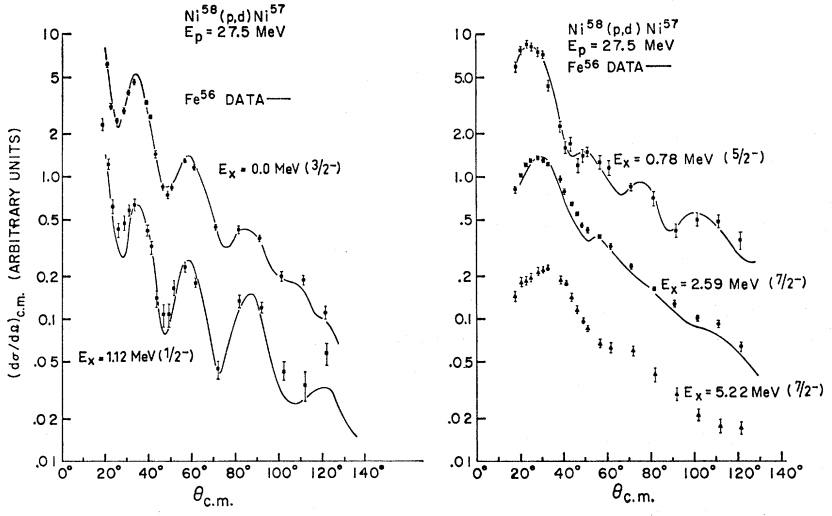

FIG. 6. Angular distributions of deuterons from the $Ni^{58}(p,d)Ni^{57}$ reaction at 27.5 MeV, with arbitrary normalization. The lines through the Ni^{58} data points are taken from the Fe^{56} data at the same energy.

[30] R. H. Fulmer and W. W. Daehnick, Phys. Rev. 139, B579 (1965).

C. $C^{12}(p,d)C^{11}$

Since the Q value for the $C^{12}(p,d)C^{11}$ reaction is -16.5 MeV, only the first four states could be seen at a proton energy of 27.5 MeV. Angular distributions are shown in Fig. 7 for these levels at excitations of 0.0 ($\frac{3}{2}^-$), 2.0 ($\frac{1}{2}^-$), 4.32 ($\frac{5}{2}^-$), and 4.81 MeV ($\frac{3}{2}^-$).[31] There are, indeed, large differences between the $\frac{3}{2}^-$ and $\frac{1}{2}^-$ patterns; a comparison of the back-angle data for the first two states, for example, reveals the same sort of dip in the $\frac{1}{2}^-$ cross section that was seen in the $2p$ shell distributions described above. However, it is not clear that this is a J-dependent effect and not a Q-dependent one. Figure 8 compares the carbon data with preliminary data for $O^{16}(p,d)O^{15}$ at the same energy. The C^{11}, $Q=-21.3$ MeV, $\frac{3}{2}^-$ distribution is quite different from the C^{11}, $Q=-16.5$ MeV $\frac{3}{2}^-$ curve, but it is very similar

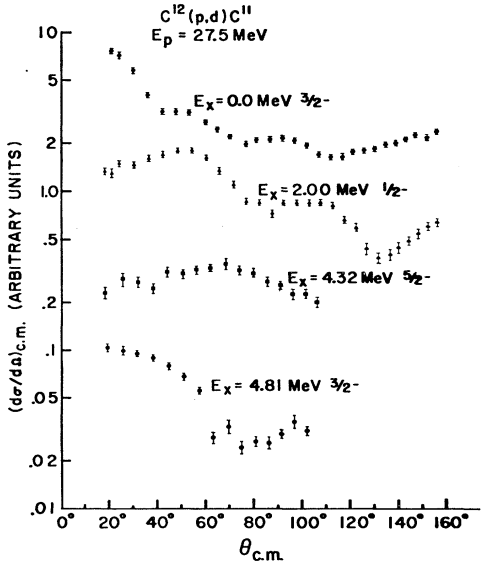

FIG. 7. Angular distributions of deuterons from the $C^{12}(p,d)C^{11}$ reaction at 27.5 MeV, with arbitrary normalization.

to the O^{16}, $Q=-19.6$ MeV, $\frac{3}{2}^-$ curve whose Q value is much closer. Likewise, the two $\frac{1}{2}$ distributions are remarkably dissimilar, but their Q values differ by 5 MeV. The interpretation that at least the forward angle differences are Q effects is reinforced by the data of Kelly *et al.*[32] at 36 MeV. They found that the ground-state and 2.00-MeV distributions were almost identical from 15°–70°. The 40-MeV data of Kavaloski *et al.*[21] for the C^{11} ground state and the O^{15} ground state and 6.16-MeV state also show very similar forward-angle distributions. Back-angle data were not reported.

D. $S^{32}(p,d)S^{31}$

The $l=2$ transfers to the $\frac{3}{2}^+$ state at 1.24 MeV and the $\frac{5}{2}^+$ state at 2.23 MeV in S^{31} were studied with

[31] A. S. Rupaal, B. L. White, and J. R. Prescott, Bull. Am. Phys. Soc. 8, 119 (1963).
[32] William H. Kelly, Carl A. Ludemann, and Charles D. Goodman, Bull. Am. Phys. Soc. 10, 121 (1965).

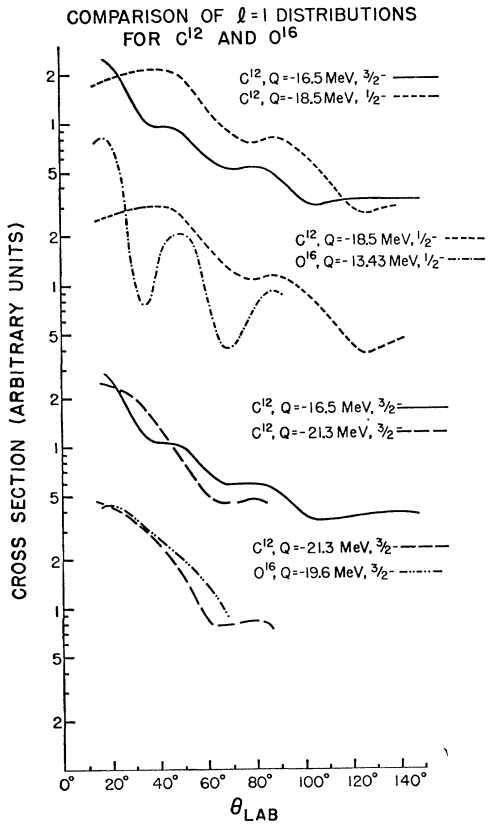

FIG. 8. Comparison of $C^{12}(p,d)C^{11}$ data with preliminary data for $O^{16}(p,d)O^{15}$; the proton energy is 27.5 MeV.

28-MeV protons. Sulfur targets, prepared by condensing sulfur vapor on water and coating the surface of the dried film with polystyrene, tended to evaporate under proton bombardment. Thus, only the scintillation counter monitor placed at 90°, where the C^{12} and S^{32} elastic peaks were clearly separated, could be used to

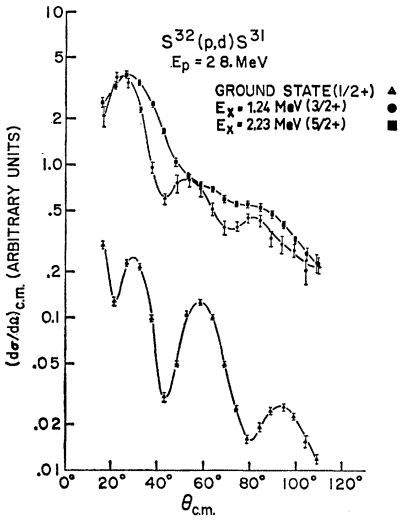

FIG. 9. Angular distributions of deuterons from the $S^{32}(p,d)S^{31}$ reactions at 28 MeV, with arbitrary normalization.

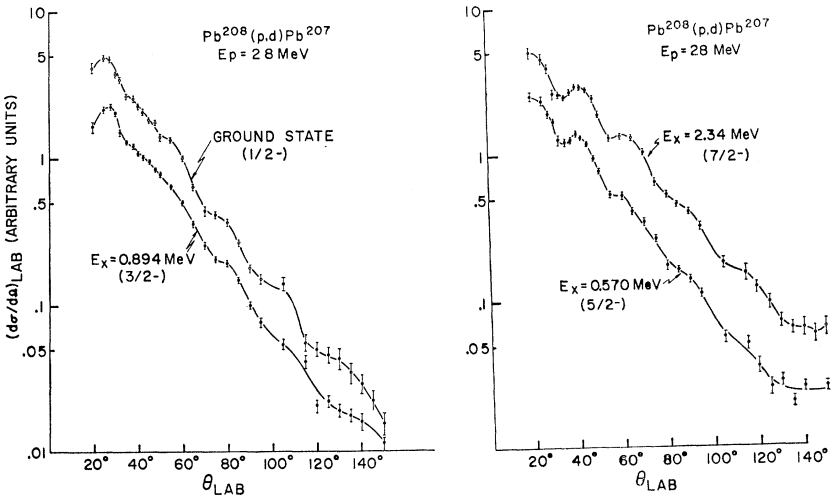

FIG. 10. Angular distributions from the $Pb^{208}(p,d)Pb^{207}$ reaction at 28 MeV, with arbitrary normalization. Data for $l=1$ transfer are shown on the left, data for $l=3$ on the right.

compute the cross sections. The (p,d) cross section at 30° was remeasured at regular intervals during the run as a check against normalization errors.

Angular distributions for these states have been reported previously by Kavaloski *et al.*[21]; their proton energy was 40 MeV and their distributions extended from 5°–60°. There is a small shift of a few degrees apparent between their $\frac{3}{2}^+$ and $\frac{5}{2}^+$ curves; otherwise the two are quite parallel. On the other hand, the present data, shown in Fig. 9, reveal a J dependence which is quite similar to the J dependence seen in $l=3$ transfers in Fe and Ni at 27.5 MeV. In fact, it is more difficult to distinguish the $\frac{5}{2}^+$ from the $\frac{7}{2}^-$ or the $\frac{3}{2}^+$ from the $\frac{5}{2}^-$ than it is to distinguish between the $\frac{3}{2}^+$ and $\frac{5}{2}^+$ or between the $\frac{5}{2}^-$ and $\frac{7}{2}^-$. Likewise, the J dependence that is seen here in $S^{32}(p,d)S^{31}$ with outgoing deuteron energies of about 14 MeV is similar to that seen for $l=2$ transfer in $S^{32}(d,p)S^{33}$ at $E_d=12$ MeV by Schiffer *et al.*[10] But it is much more definite than the $l=2$ J dependence observed in (p,d) on the Sn isotopes at 30 MeV by Cavanagh *et al.*[15]

E. $Pb^{208}(p,d)Pb^{207}$

The $2f$ and $3p$ shells are both filled in Pb^{208}, so that the (p,d) reaction can easily reach the $\frac{1}{2}^-$, $\frac{3}{2}^-$, $\frac{5}{2}^-$, and $\frac{7}{2}^-$ neutron-hole states in Pb^{207}. With protons of 28 MeV and with a ground state Q-value of -5.15 MeV, the outgoing deuterons are sufficiently energetic that the high Coulomb barrier does not make the cross section small. No previous studies of J dependence in this mass region have been reported. The $Pb^{206}(d,p)Pb^{207}$ data of Cohen *et al.*,[33] taken with 15-MeV deuterons, show large Coulomb effects; their curves for all states are relatively flat out to about 90°. Data of Erskine and Siemssen[34] on $W^{182}(d,p)W^{183}$ at $E_d=12$ MeV show very slight differences between $\frac{5}{2}^-$ and $\frac{7}{2}^-$ curves; again, the lack of a forward peak indicates that Coulomb barrier effects are dominant at this energy.

The angular distributions obtained in the present (p,d) work at 28 MeV are shown in Fig. 10. Both $l=1$ and $l=3$ curves are forward peaked, but in none is the structure very pronounced. The slopes of the curves for the same l value but different J values are just about identical, and there are certainly no striking differences in shape between them. There is some hint of structure in the $\frac{1}{2}$ that is not found in the $\frac{3}{2}$, and of slight phase differences between the $\frac{5}{2}$ and $\frac{7}{2}$. However, the J dependence is definitely not comparable to the effects seen for the same angular momentum transfer in Fe^{56} and Ni^{58}. On the other hand, it is still quite easy to distinguish between different l values; the $l=1$ and $l=3$ curves are noticeably different.

F. $Fe^{56}(He^3,\alpha)Fe^{55}$

The (He^3,α) reaction on Fe^{56} was first studied by Blair and Wegner[35] at an energy of 14.3 MeV, with insufficient resolution to confidently separate the $\frac{3}{2}^-$

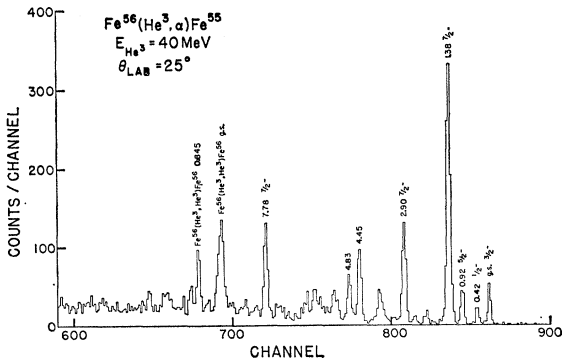

FIG. 11. A spectrum of alpha particles at 25° from the $Fe^{56}(He^3,\alpha)Fe^{55}$ reactions at 40 MeV. Some elastically scattered He^3 particles are also visible. Excitation energies and spins refer to Fe^{55} unless otherwise noted.

[33] B. L. Cohen, R. E. Price, and S. Mayo, Nucl. Phys. **20**, 370 (1960).

[34] J. R. Erskine, Phys. Rev. **138**, B66 (1965); L. L. Lee, Jr. and J. P. Schiffer, *ibid.* **136**, B405 (1964).

[35] A. G. Blair and H. E. Wegner, Phys. Rev. **127**, 1233 (1962).

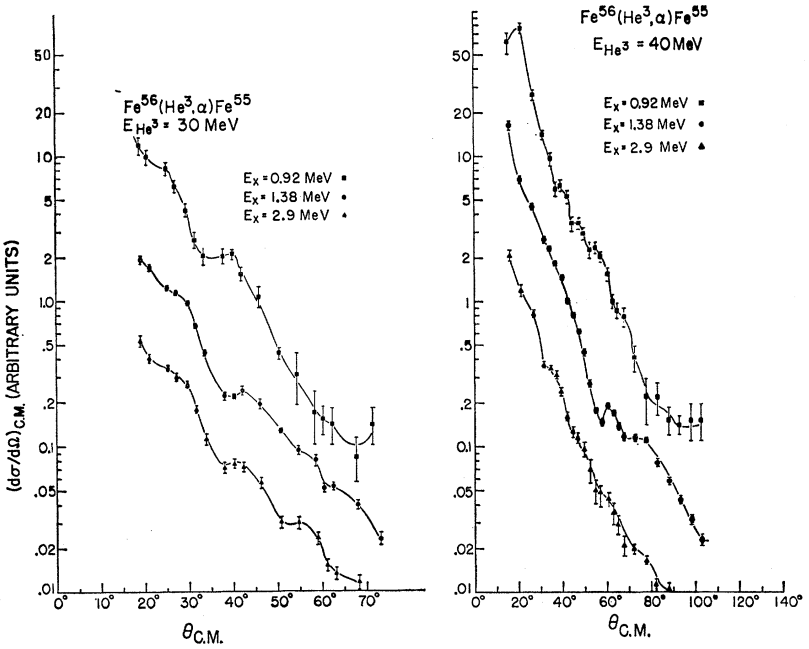

FIG. 12. Angular distributions of alpha particles from the $Fe^{56}(He^3,\alpha)Fe^{55}$ reaction at 30 MeV, on the left, and at 40 MeV, on the right. Note that the angular scale is not the same for the two energies.

ground state from the $\frac{1}{2}^-$ 0.42-MeV state, or the 0.92-MeV $\frac{5}{2}^-$ state from the 1.38-MeV $\frac{7}{2}^-$ state. Mayer-Böricke *et al.*[7] have found evidence for J dependence in this reaction at 17.5 MeV, but the differences between states of the same l and different J are not striking. The same is true of the Ni^{60} and Ni^{62} (He^3,α) results at 24.5 MeV reported by Brussel *et al.*[8] The present data were taken at incident energies of about 30 and 40 MeV.

An energy spectrum of alphas at 25° from the 40-MeV run is depicted in Fig. 11. The spectrum was taken with a multiplier, but the window was set sufficiently wide that some He^3 particles were allowed to gate the analyzer. Note that the same states are excited as in (p,d), but the $l=3$ cross sections are enhanced relative to $l=1$ cross sections, as noted previously.[35] Consequently, the statistics on the $l=1$ data are quite poor and hardly adequate to make any statements about J dependence; these data are not shown here. On the other hand, there are definite differences between the 0.92-MeV $\frac{5}{2}^-$ and the 1.38-MeV $\frac{7}{2}^-$ distributions both at 30 and 40 MeV, illustrated in Fig. 12. Ratios of cross sections for these $l=3$ transitions are plotted in Fig. 13.

The $l=3$ (He^3,α) distributions are quite structureless. The differences between $\frac{5}{2}^-$ and $\frac{7}{2}^-$ distributions are mostly phase differences, and they become noticeable only on the ratio plot. Structure is found in the $(\frac{5}{2}^-)/(\frac{7}{2}^-)$ ratio at both 30 and 40 MeV; the peaks in the ratio occur at different angles at the two energies. The fact that the ratio of the two $\frac{7}{2}^-$ states is not a constant either, however, means that either the structure of the states or the Q value plays some role in determining $\sigma(\theta)$. Nevertheless, the Q dependence does not seem sufficient to explain the J dependence, since the $(\frac{5}{2})/(\frac{7}{2})$ ratio shows considerably more structure than the $(\frac{7}{2})/(\frac{7}{2})$, though the difference in Q is smaller. The J dependence still is not striking, however; more systematics are needed to make this reaction a reliable J indicator.

IV. DISCUSSION AND COMPARISON WITH THEORY

In trying to account for the J dependence observed in the (p,d) and (He^3,α) reactions described above, it is clear that a spin-orbit force should be considered first. The $\mathbf{l}\cdot\mathbf{s}$ forces acting on the bound neutron are very strong and generally well known. Since they are attractive for $l+\frac{1}{2}$ and repulsive for $l-\frac{1}{2}$ neutrons, the potential well which binds an $l-\frac{1}{2}$ neutron by a given amount must be deeper than the well which binds an $l+\frac{1}{2}$ neutron by the same amount. On the other hand, since it is a surface potential, it will tend to make the $l+\frac{1}{2}$ wave function peak at a larger radius than the $l-\frac{1}{2}$ wave function. These differences in the form factors can produce a J dependence in the DWBA prediction when the spin-orbit potential is strong enough. However, such a model predicts that the differential cross section for pickup of the higher spin neutron will be peaked at an angle slightly more forward than the distribution for pickup of the lower spin neutron, contrary to observation. To counteract this effect of the spin-orbit force, and to explain some other results, it has been proposed that one should use an effective binding energy for the neutrons, such that the energy separation between $l+\frac{1}{2}$ and $l-\frac{1}{2}$ single particle states is preserved. The decreased binding for the lower spin particle spreads its wave function to larger radii. Sherr *et al.*[2] chose an effective binding for $\frac{5}{2}^-$ neutrons 6 MeV less than the separation energy of $\frac{7}{2}^-$ neutrons. The corresponding

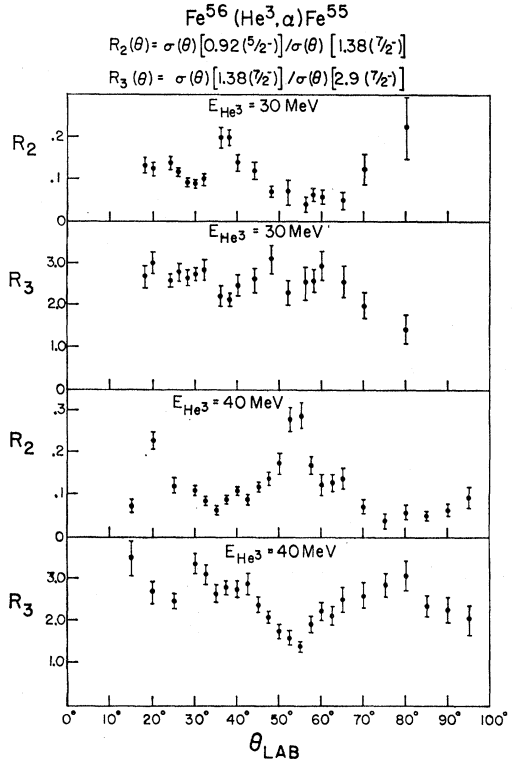

FIG. 13. Cross section ratios for $l=3$ transfer in the $Fe^{56}(He^3,\alpha)$ reaction. The ratio of the $\frac{5}{2}^-$ to the $\frac{7}{2}^-$ cross section at 30 MeV is shown in the top box, and at 40 MeV in the third box. The ratios of two $\frac{7}{2}^-$ cross sections are shown in the second and fourth boxes at 30 and 40 MeV, respectively.

DWBA predictions gave a good account of the forward angle $l=3$ J-dependent distributions.

It is well known that the use of such an effective binding can be criticized on the grounds that the asymptotic form of the wave function has the wrong shape. Moreover, Austern[36] and Pinkston and Satchler[37] have discussed the influence of residual interactions and configuration mixing on the radial shape of zero-order single-particle wave functions. Even when only two particles in a $(j)^2$ configuration are considered, the shape as well as the magnitude of the potential well are modified in a way that is difficult to predict. In the absence of more exact calculations, the latter authors agree that phenomenological models should be used, but they would prefer, e.g., a well of increased radius for the $\frac{5}{2}^-$ neutron rather than an effective binding energy to explain J dependence. The resulting form factor is quite similar to the effective binding form factor, but it has the correct asymptotic decay; the change in the well is reasonable on the basis of a vibrational model with a surface localization of the interaction between the odd neutron and the core. It will be interesting to compare both this prescription and the effective binding prescription with the data of Sec. III. More recently, Huby and Hutton[38] have undertaken more exact calculations of the effect of residual interactions on the $\frac{5}{2}^-$ wave function in Ni^{57}. Their form factors are quite similar to the phenomenological ones examined here, and give much the same differential cross sections in the case reported.

Spin-orbit forces acting on the incoming or outgoing projectiles must also be considered in trying to explain J dependence. Greider[39] has used a diffraction model with spin-orbit coupling of this type to fit some results; more recently, Pearson and Coz[40] have suggested that the polarization of elastically scattered protons is intimately connected with $l=1$ J dependence in the (d,p) reaction. Only a small number of DWBA calculations have been published in which a spin-orbit potential has been included in an attempt to fit J dependence. In their extensive analysis of the Ca^{40}-$(d,p)Ca^{41}$ reaction, Lee *et al.*[41] found that spin-orbit coupling tended to put a dip in the predicted $\frac{1}{2}^-$ angular distribution, at about the correct angle, but it also put a dip in the $\frac{3}{2}^-$ curve that was not experimentally observed. Further, with different sets of optical parameters that fit the elastic scattering, the $\frac{1}{2}^-$ dip would disappear. A later calculation reported by Satchler[42] gave quite a good fit to both $\frac{3}{2}^-$ and $\frac{1}{2}^-$ curves. The best evidence that the spin-orbit interaction can provide a good explanation for J dependence comes from the (α,p)[4] and (p,α)[5] reactions in which it can affect only the proton. With parameters that fit the elastic scattering, the DWBA definitely predicts that the $\frac{1}{2}^-$ should have more structure than the $\frac{3}{2}^-$, provided that the radial integration has a lower cutoff at the nuclear surface. Such a prediction is in good agreement with the data, although the angular positions of the predicted minima in the $\frac{1}{2}^-$ are sensitive to small changes in the real central potential.

A. DWBA Calculations

To provide a stringent test of the proposed explanations of J dependence, DWBA calculations for the $Fe^{56}(p,d)Fe^{55}$ reaction were carried out over the energy range from 18.5–27.5 MeV, using the Oak Ridge computer code JULIE.[43] Many of these calculations included the effects of the finite range of the neutron-proton interaction, and the effects of nonlocality of the optical- and shell-model potentials. The latter calculations made use of the local energy approximation (LEA), which has been tested by Dickens *et al.*,[44] and was found to give

[36] N. Austern, Phys. Rev. **136**, B1743 (1964).
[37] W. T. Pinkston and G. R. Satchler, Nucl. Phys. **72**, 641 (1965).
[38] R. Huby and J. L. Hutton, Phys. Letters **19**, 660 (1966).
[39] K. R. Greider, Phys. Rev. **136**, B420 (1964).
[40] C. A. Pearson and M. Coz, Nucl. Phys. **82**, 533 (1966).
[41] L. L. Lee, Jr., J. P. Schiffer, B. Zeidman, G. R. Satchler, R. M. Drisko, and R. H. Bassel, Phys. Rev. **136**, B971 (1964).
[42] G. R. Satchler, Argonne National Laboratory Report No. ANL-6878, p. 23 (unpublished).
[43] We are grateful to Dr. R. M. Drisko for making this program available to us.
[44] J. K. Dickens, R. M. Drisko, F. G. Perey, and G. R. Satchler, Phys. Letters **15**, 337 (1965).

TABLE I. Optical parameters used in DWBA calculations. Column 2 gives the energy range over which the parameters were used. The remaining columns refer to the parameters of an optical potential of Woods-Saxon shape (see Ref. 46). [W_D (this work) $=4W_D$ (Ref. 46)]. The parameters V_S and W_D were varied smoothly within the range specified as a function of energy.

Label	E (MeV)	V_S (MeV)	r_{0S} (F)	a_S (F)	W_S (MeV)	W_D (MeV)	r_I (F)	a_I (F)	V_{SO} (MeV)
				A. Proton parameters					
$P1$[a]	18.5–27.5	47.7–42.8	1.25	0.65	0.0	47.2–44.0	1.25	0.47	8.0
$P2$[b]	18.5–27.5	55.0–50.0	1.18	0.70	0.0	50.0–35.0	1.04	0.68	7.5
$P3$[c]	18.5–27.5	47.7–44.5	1.25	0.65	0.0	30.0	1.25	0.70	5.5
$P4$[d]	27.5	44.69	1.19	0.69	2.16	26.0	1.19	0.65	6.7
$P5$[d]	27.5	40.52	1.25	0.65	12.55	0.0	1.25	0.47	6.0
				B. Deuteron parameters					
$D1$[e]	8.0–18.0	97.0–91.5	1.15	0.81	0.0	78.0	1.34	0.68	0.0
$D2$[e]	8.0–18.0	52.0–44.0	1.30	0.79	0.0	67.6–60.0	1.37	0.67	0.0
$D3$[e]	9.0–14.0	57.0–55.0	1.18	0.87	0.0	68.0–64.0	1.36	0.68	0.0
$D4$[f]	9.0	93.0	1.20	0.42	0.0	32.4	1.36	0.99	0.0

[a] See Ref. 45. [b] See Ref. 46. [c] See Ref. 47. [d] See Ref. 48. [e] See Ref. 49. [f] See Ref. 50.

results very similar to those obtained with an exact finite-range code under many conditions. A range of 1.25 F was used for the neutron-proton interaction; the nonlocality parameters were set at 0.85 and 0.54 for nucleons and deuterons, respectively.

Table I[45–50] lists the various sets of optical parameters used in these calculations. They refer to a potential of the standard Woods-Saxon form. All the parameters have been taken from standard optical-model analyses, which generally included an attempt to find sets of geometrical parameters which gave very good fits over a large energy and mass region, rather than widely varying best-fit sets. This type of analysis is ideally suited to our study of the DWBA predictions of J dependence for the $Fe^{56}(p,d)Fe^{55}$ data since, as much as possible, it isolates the energy dependence inherent in the DWBA from that associated with fluctuating optical parameters.

The spin-orbit term presents some problems. A real surface form was used throughout; no volume or imaginary terms were included. The parameters of the spin-orbit term had to be kept the same as those of the real central term; there is now good evidence, however, that the spin-orbit radius and diffuseness should be somewhat smaller than the corresponding central parameters.[51] The strength of the spin-orbit term is quite well known for protons, but its value for deuterons is not well determined. The figure of 8 MeV that has been generally used here is probably an overestimate.

B. Predictions for $l=1$ Transfer

Most analyses of stripping and pickup reaction data have made use of the zero range approximation and local potentials. Typical fits of this type (henceforth called LZR) to the $l=1$ $Fe^{56}(p,d)Fe^{55}$ angular distributions are shown in Fig. 14. The standard Perey potentials ($P1$ and $D1$ of Table I) were used at all the energies; they include a spin-orbit potential of 8 MeV acting on the protons but not on the deuterons. The geometrical parameters of the neutron form factor were also standard ($N1$ of Table II).

It is clear from this figure that the dashed curves, which are calculated with a lower cutoff (CO) on the radial integration at 4.75 F, give a much better fit than the solid curves which are calculated without such a cutoff (henceforth called NCO). The data have been normalized to the CO curves at the second maximum; the relative normalization of the CO and NCO curves is that predicted by the DWBA. The $\frac{3}{2}^-$ distributions are, in fact, fit quite well by the CO curves, at least at 22.4 MeV and above. The NCO patterns do not contain enough oscillations at these energies; this behavior was consistently repeated in calculations with many potentials in addition to the one illustrated here. Even the CO curves do not fit the $\frac{1}{2}^-$ data very well at any energy, but they do have deeper minima and larger maxima than the NCO curves, which is in accord with the experimental distributions.

TABLE II. Geometrical parameters of the potential well binding the picked-up neutron. Column 2 gives the radius parameter (the nuclear radius is $r_0A^{1/3}$) and column 3 gives the diffuseness of a Woods-Saxon type potential.

Label	r_0 (F)	a (F)
$N1$	1.25	0.65
$N2$	1.35	0.65
$N3$	1.50	0.65
$N4$	1.15	0.65
$N5$	1.05	0.65

[45] F. G. Perey, Phys. Rev. **131**, 745 (1963).
[46] M. P. Fricke and G. R. Satchler, Phys. Rev. **139**, B567 (1965).
[47] Louis Rosen, Jerome G. Beery, Alfred S. Goldhaber, and Elliot H. Auerbach, Ann. Phys. (N.Y.) **34**, 96 (1965).
[48] R. C. Barrett, A. D. Hill, and P. E. Hodgson, Nucl. Phys. **62**, 133 (1965).
[49] J. K. Dickens and F. G. Perey, Phys. Rev. **138**, B1083 (1965).
[50] William R. Smith, Phys. Rev. **137**, B913 (1965).
[51] F. G. Perey, in *Proceedings of the Second International Symposium on Polarization Phenomena of Nucleons, Karlsruhe, 1965* (Birkhäuser Verlag, Basel, Switzerland, 1966); L. J. B. Goldfarb, G. W. Greenlees, and M. B. Hooper, Phys. Rev. **144**, 829 (1966); D. J. Baugh, J. A. R. Griffith and S. Roman, Nucl. Phys. **83**, 481 (1966).

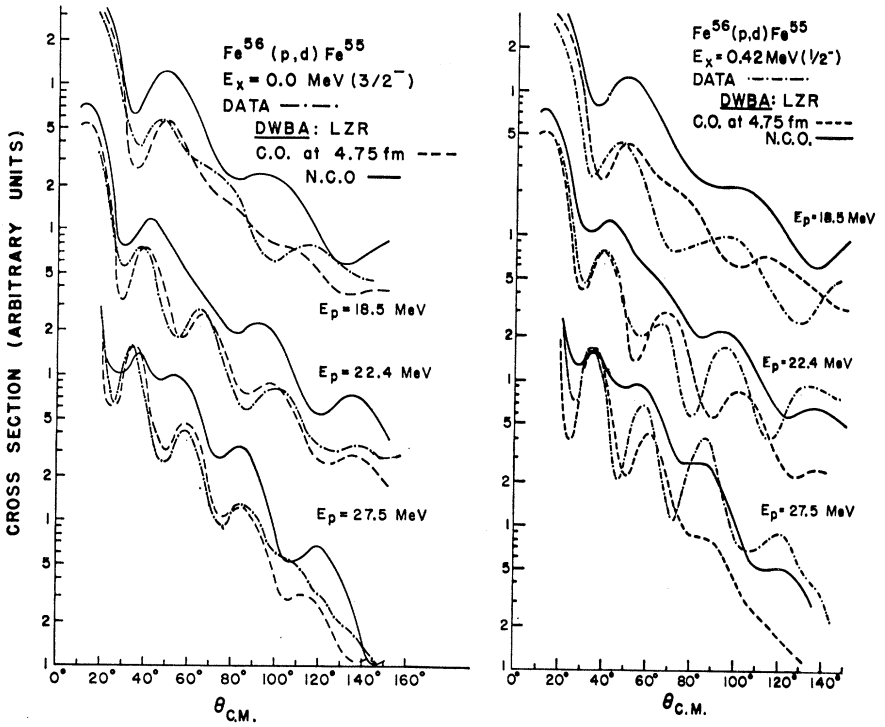

FIG. 14. Comparison of the data for $l=1$ transfer in the Fe^{56}-$(p,d)Fe^{55}$ reaction with local, zero-range DWBA calculations at several energies. The experimental data have been normalized to match the CO calculations at the second maximum, but the relative normalization of the NCO and CO curves is predicted by the DWBA.

These conclusions are not modified when the calculations are carried out with finite range and nonlocal potentials (FRNL). Figure 15 depicts FRNL calculations for the ground-state transition at three energies and compares them with LZR calculations. The specifically FRNL effects are just about the same for $\frac{1}{2}^-$ transitions and so are not illustrated. The relative normalization of the four curves at each energy is that predicted by the DWBA, but the absolute value of any one set is arbitrary. Generally, the FRNL curves fall between the NCO and CO versions of the LZR curves. The FRNL predictions without a cutoff have quite a bit more structure than the corresponding LZR predictions, and so they give a better fit to the data. However, they still do not match the $l=1$ experimental distributions nearly as well as the CO curves do. The latter have almost the same shapes for both LZR and FRNL, but the maximum at about 40° tends to be higher with FRNL than LZR. The fit to the $\frac{1}{2}^-$ remains poor.

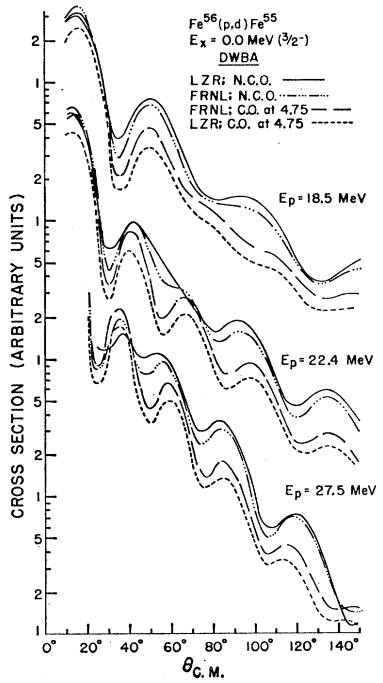

FIG. 15. Comparison of local, zero range and nonlocal, finite range DWBA calculations for the $\frac{3}{2}^-$ state in Fe^{55}.

The addition of a spin-orbit term to the deuteron optical potential does not improve this situation. In fact, the spin-orbit terms in both the proton and the deuteron optical potentials were found to have an influence on the calculated distributions which was small and did not necessarily improve the quality of the fit to the data. Figure 16 shows $\frac{3}{2}^-$ and $\frac{1}{2}^-$ predictions plotted together with the data at three energies. A spin-orbit strength of 8.0 MeV was used here for both protons and deuterons; the other potential parameters were not adjusted to make up for the addition of this term to the deuteron potentials.

As these figures show, the DWBA predicts a small $l=1$ J dependence, which is usually a slight difference in phase rather than the very pronounced differences in shape and structure that are observed in the $l=1$ data. To determine whether these poor results could be ascribed to the optical-model parameters chosen, the other potentials listed in Table I were also tried. The

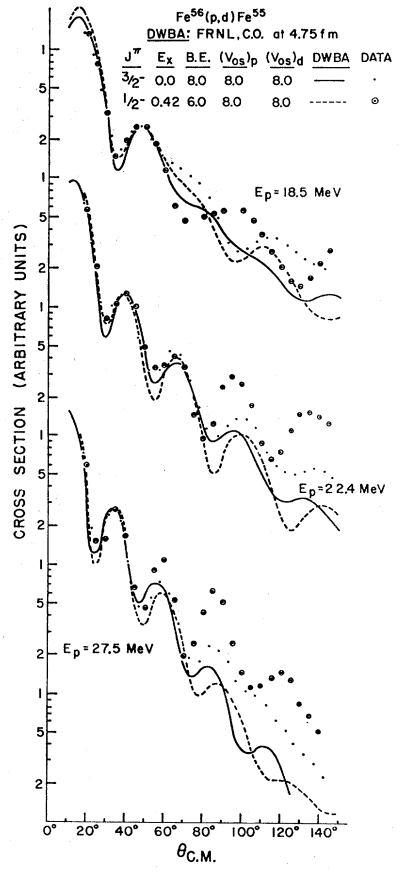

FIG. 16. Finite range, nonlocal DWBA calculations for $l=1$ transitions in $Fe^{56}(p,d)Fe^{55}$. A spin-orbit strength of 8 MeV is included in both the proton and the deuteron optical model potentials.

deuteron spin-orbit potential was varied over a wide range. These changes sometimes produced distributions somewhat different in shape from those of Fig. 16, but the actual J dependence predicted was very little different from that predicted with $P1$ and $D1$. This is contrary to the observation of Lee *et al.*,[41] who found that the influence of spin-orbit potentials on the distributions predicted for the $Ca^{40}(d,p)Ca^{41}$ reaction depended critically on the other parameters.

C. Predictions for $l=3$ Transfer

For the $l=3$ distributions in Fe^{56}, NCO calculations do better than CO, but neither fits the data very well over the entire energy range. LZR predictions with the standard Perey parameters for the $\frac{5}{2}^-$ 0.92-MeV and $\frac{7}{2}^-$ 1.38-MeV states are shown in Fig. 17. The CO curves probably give almost as good a fit as the NCO curves in the forward direction, but they fall off much too rapidly at the large angles and predict too large an angular shift in the forward peak as the energy changes. The gross features of the observed distributions are matched reasonably well by the NCO curves, notably the angular shift and widening of the first maximum as the energy decreases. Even this maximum is not fit well quantitatively for either state, however. The predictions for the $\frac{7}{2}$ and $\frac{5}{2}$ are just about the same in shape and structure; they tend to fall between the two observed distributions, closer to the $\frac{7}{2}$ at high energy, closer to the $\frac{5}{2}$ at low energy.

Introduction of nonlocality and finite range into the $l=3$ calculations brings about changes which are significant from the point of view of J dependence at the high energies. Fig. 18 illustrates this result. At angles

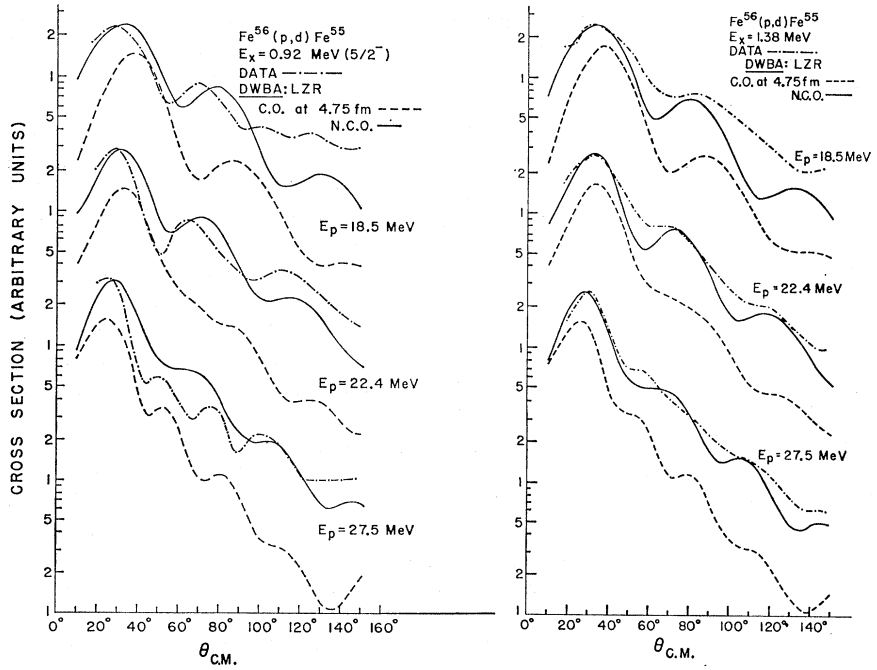

FIG. 17. Comparison of the data for the $Fe^{56}(p,d)$ reaction to $\frac{5}{2}^-$ and $\frac{7}{2}^-$ states in Fe^{55} with local, zero range DWBA calculations. The experimental data have been normalized to match the NCO calculations at the first maximum, but the relative normalization of the NCO and CO curves is that predicted by the DWBA.

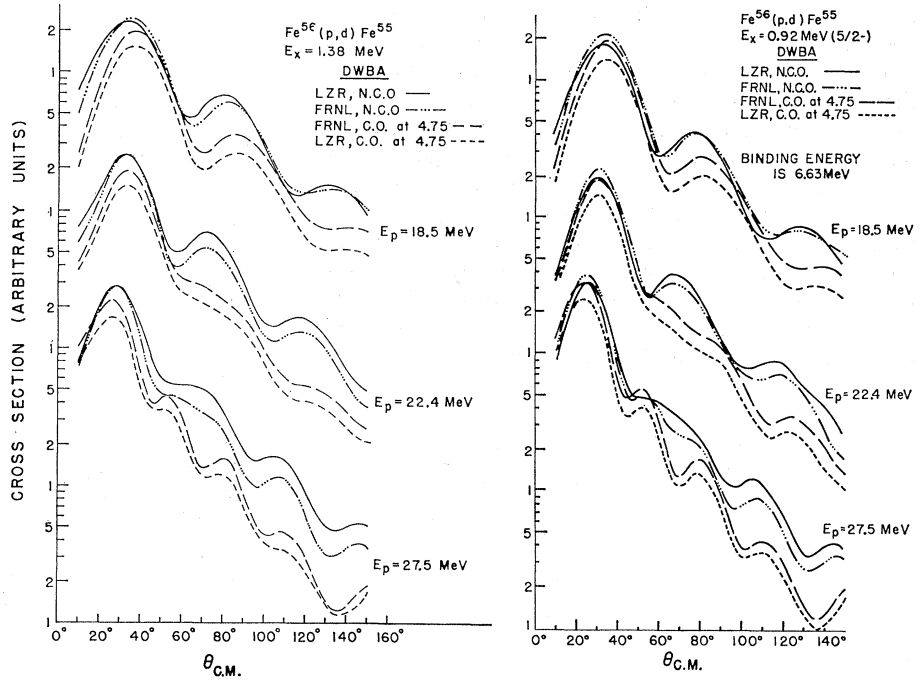

FIG. 18. Comparison of local, zero range, and nonlocal, finite range DWBA calculations for $l=3$ transitions in $Fe^{56}(p,d)$-Fe^{55}. The $\frac{5}{2}^-$, 0.92-MeV curve, shown on the right, is calculated with an effective binding energy.

past 60° the $\frac{7}{2}^-$ FRNL curve is reduced in magnitude relative to the LZR curve, but it has about the same shape; in the forward angles, however, the FRNL curve decreases more quickly from the forward maximum than the LZR curve. This is unfortunate since the LZR curve had given an excellent fit to the $\frac{7}{2}^-$ data at 27.5 MeV. The $\frac{5}{2}^-$ curves calculated with the standard separation energy (SE) for the neutron (not illustrated) show a similar change due to FRNL, but the $\frac{5}{2}^-$ curves calculated with an effective binding energy (EB) of 6.63 MeV for the neutron are not so affected (see Fig. 18). Thus, whatever differences there were between the $\frac{7}{2}^-$ and EB $\frac{5}{2}^-$ predictions in LZR at 27.5 MeV have been significantly decreased in the FRNL calculation. This is discussed at greater length below. At the lower energies, FRNL has a gradually decreasing effect on the forward maximum, so that at 22.4 MeV there is no difference in this region between LZR and FRNL calculations.

The effective binding prescription had been proposed by Sherr *et al.*[2] to explain the J dependence results at 27.5 MeV; we have mentioned also that Pinkston and Satchler[37] suggested a change in radius of the neutron well as a better solution. The results of calculations with these two form factors are illustrated in the succeeding figures. All are FRNL calculations. Figure 19 reveals that the use of the EB form factor does indeed make an improvement in the quality of the fit to the $\frac{5}{2}^-$ over the forward maximum that is significant at all energies, although the change is somewhat smaller at the lower energies. At 27.5 MeV the improvement is sufficient to give an excellent fit to the forward-angle data, but at lower energies the data are still shifted by about 5° to the left of the predictions. At the backward angles, which are not shown, the fit is much worse than this; the DWBA distributions calculated with effective binding decrease more rapidly than those calculated with separation energy binding, and the latter decreased too quickly already. Figure 20 shows that the use of a form factor computed for a potential well of greatly increased radius has only a small effect on the predicted angular distributions. In fact, except at the two highest energies, there is only a negligible difference over the forward maximum between the calculations with the two different neutron radii.

The change in the radius of the form factor has an influence on the $\frac{7}{2}^-$ predictions similar to that just mentioned for the $\frac{5}{2}^-$, as shown in Fig. 21. At high energy, the effect of the smaller radius is appreciable, enough to give a good fit to the data. But at lower energies the change in radius has a negligible effect, so that we are left with a substantial discrepancy between the prediction and the experiment. Notice, in fact, that at 18.5 MeV the change in radius of the form factor produces a change in $\sigma_{\mathrm{DWBA}}(\theta)$ that is opposite from that expected for both the $\frac{5}{2}^-$ and the $\frac{7}{2}^-$.

Now the effective binding prescription predicted at least some J dependence at all energies, although the fits, especially at lower energy, were not good. To examine this proposal more closely, the correct separation energy tail was joined to an effective binding form factor at various radii. The results of an LZR calculation with this combination form factor at 27.5 MeV are shown in Fig. 22. The differences between SE and EB calculations were greater in LZR than in FRNL; the LZR calculation thus shows the effect of the cor-

rected tail more clearly. The curves in Fig. 22 have all been normalized to the same height at the peak. Note that the shape of the tail at radii larger than 9 FM has little effect on the predicted curve; the solid and dashed lines overlap very well. However, when the SE tail is joined at 7 or at 5 F, the predicted angular distribution is changed considerably. Indeed, the curve calculated with the EB form factor to 5 F and the SE form factor thereafter is identical at angles less than 40° with the curve determined entirely by the separation energy; at larger angles it does drop off slightly more than the SE curve. Thus, joining the correct tail to an EB form factor does not improve the fit to J

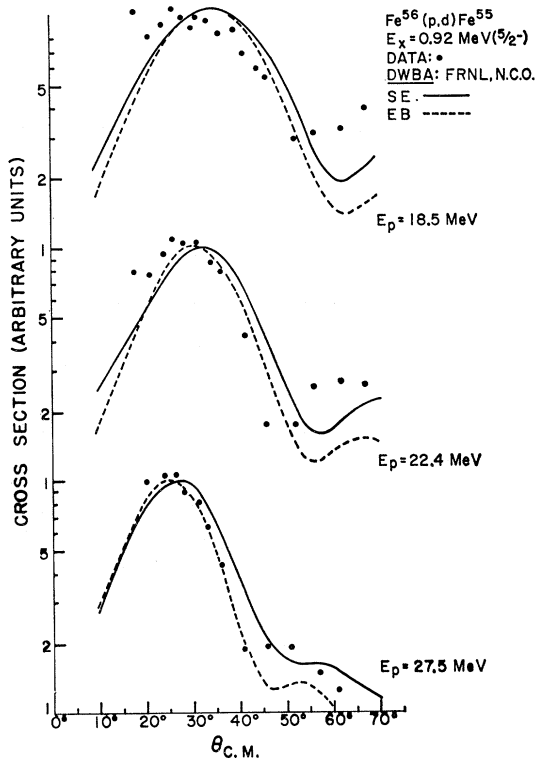

FIG. 19. Comparison of DWBA calculations for $\frac{5}{2}^-$ state in Fe^{55} using separation energy binding (SE) for the picked-up neutron with calculations using an effective binding (EB) energy of 6.63 MeV.

dependence; on the contrary, it makes the fit worse and reveals that much of the difference between SE and EB calculations arises from the region where the nuclear potential is small. This is the region where the wave function should begin to take on its asymptotic form, viz., the SE form.

It would be interesting to conclude from this discussion that the shape of the form factor inside the nucleus has no effect on the shape of the first maximum in $l=3$ distributions, and thus that modifications to the nuclear potential seen by $\frac{5}{2}$ and $\frac{7}{2}$ particles cannot provide an explanation for J dependence. However, we

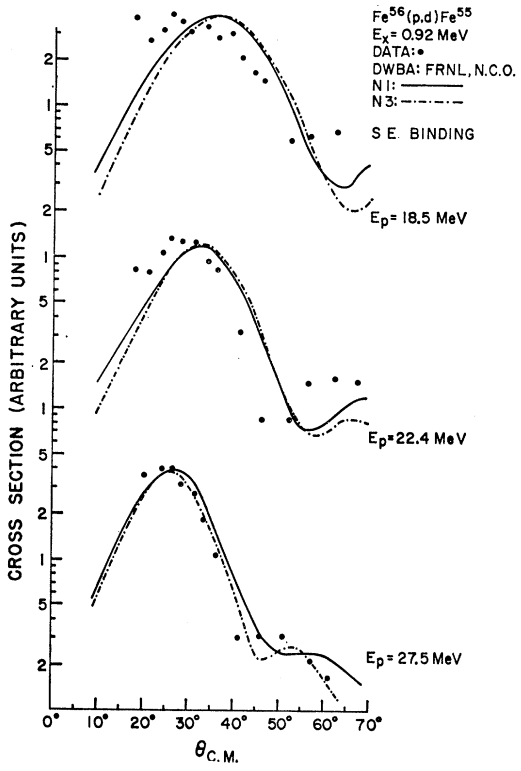

FIG. 20. The effect of a change in the radius of the potential well on the DWBA predictions for the $\frac{5}{2}^-$ state in Fe^{55}. The label $N1$ refers to an assumed radius parameter of 1.25, while $N3$ refers to a radius parameter of 1.50.

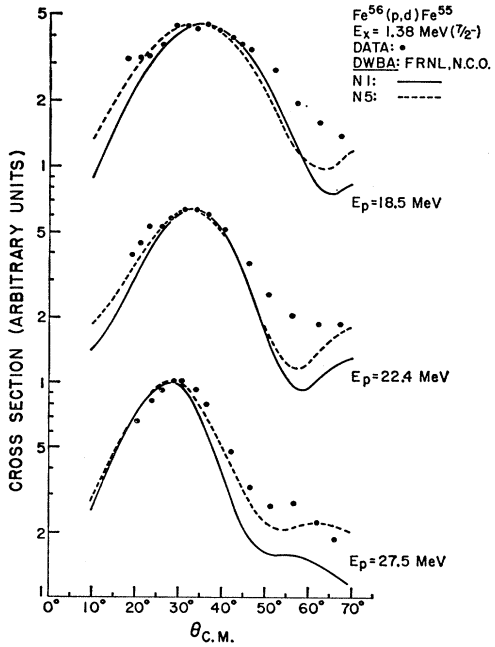

FIG. 21. The effect of a change in the radius of the potential well on the DWBA predictions for the $\frac{7}{2}^-$ state in Fe^{55}. The label $N1$ refers to an assumed radius parameter of 1.25, while $N5$ refers to a radius parameter of 1.05.

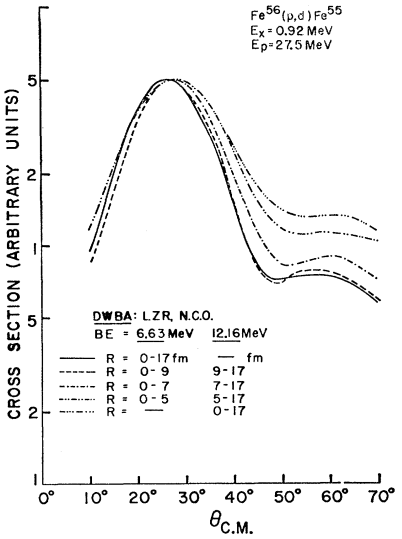

FIG. 22. DWBA calculations for the $\frac{5}{2}^-$ 0.92-MeV state in Fe^{55}, with combined form factors. The form factor was assumed to have an effective binding shape over the range specified in the left-hand column of the legend, and a separation energy shape over the rest of the range, specified in the right-hand column.

have shown only that whether the form factor has an EB or SE shape inside the nucleus does not affect the shape of this maximum, and also that rather large changes in the radius of the well do not produce the desired effect. But the form factor in the interior of the nucleus *can* affect the shape of the first maximum. To see this, we need only consider a CO prediction, which can be viewed as a calculation with a form factor which is zero in the interior. Not only do the CO distributions differ in magnitude from the NCO curves, by a factor which is energy-dependent, but they are also different in shape. Thus, if the potentials acting on either or both the $\frac{5}{2}^-$ and $\frac{7}{2}^-$ particles are radically different from the Woods-Saxon shape, as suggested by Pinkston and Satchler,[37] then it is possible that the different form factors for the two particles might produce a J dependence.

The presence of an $\mathbf{L}\cdot\mathbf{S}$ potential also offers little hope of explaining the J dependence observed in $l=3$ transfers. The DWBA does predict some differences between $\frac{5}{2}^-$ and $\frac{7}{2}^-$ curves, as shown in Fig. 23, but they do not simulate the data. A standard neutron form factor with separation energy binding, and optical potentials $P1$ and $D1$ with 8-MeV spin-orbit terms were used in these calculations. The predicted shapes of the forward maxima are essentially the same for the two values of J; what differences there are tend to be in the wrong direction. At larger angles the two curves do deviate from each other but not so as to match the experimental distributions. No hint of a more prominent second maximum for the $\frac{5}{2}^-$ can be found. Calculations performed with spin-orbit forces included in several other optical potentials consistently failed to produce any important forward angle difference between the $\frac{5}{2}^-$ and $\frac{7}{2}^-$ distributions unless the form factor was modified.

V. SUMMARY AND CONCLUSIONS

The experimental results of Sec. III are summarized briefly in Table III. The most important finding is that J dependence in the $Fe^{56}(p,d)Fe^{55}$ reaction persists over the entire energy range studied, from 18.5–27.5 MeV. The deuterons from the ground-state transition have an energy of about 18.5 MeV at the highest bombarding energy; the present data thus effectively extend the previous $l=1$ (d,p) results mentioned in Sec. I by about 4 MeV. They also show that the J dependence is not a function of the spin of the target. The forward angle $l=3$ J dependence has been observed only rarely in (d,p); the work of Alty *et al.*[13] on the Ti^{46}, Ti^{48}, and Cr^{50} (d,p) reactions, which is not without ambiguity,[29] is almost alone in the literature. The (d,p) data reported here, together with the original studies by Sherr *et al.*,[2] show, however, that spins can be determined for $l=3$ as well as for $l=1$ transitions over a large energy range. For proper identification of spins, it is, however, more important for $l=3$ than $l=1$ that the Q values of the known and unknown states whose distributions are

TABLE III. Summary of experimental results.

Reaction	(nl) of neutron	E_{inc}(MeV)	Remarks on observed J dependence
$C^{12}(p,d)C^{11}$	$1p$	27.5	Back-angle dip in 2-MeV ($\frac{1}{2}^-$) curve not seen in ($\frac{3}{2}^-$) ground-state distribution. However, neither curve is consistent with 4.8-MeV ($\frac{3}{2}^-$) curve nor with corresponding distributions in O^{16}.
$S^{32}(p,d)S^{31}$	$2d$	28.0	Distribution for $\frac{3}{2}^+$ rises to forward maximum at a smaller angle, decreases more abruptly, and has more structure than $\frac{5}{2}^+$ curve.
$Fe^{56}(p,d)Fe^{55}$, $Ni^{58}(p,d)Ni^{57}$	$2p$	18.5–27.5	At lower energies, $\frac{1}{2}^-$ and $\frac{3}{2}^-$ distributions have generally different shapes at angles larger than 50°. There are pronounced minima in $\frac{1}{2}^-$ curves at 70° and 130°, where $\frac{3}{2}^-$ are large. At higher energies, $\frac{1}{2}^-$ shows more pronounced oscillations than $\frac{3}{2}^-$ at back angles.
$Fe^{56}(p,d)Fe^{55}$, $Ni^{58}(p,d)Ni^{57}$	$1f$	18.5–27.5	Cross section for $\frac{5}{2}^-$ peaks at a more forward angle and drops off more quickly than $\frac{7}{2}^-$ at all energies. Also, $\frac{5}{2}^-$ shows more definite maxima and minima than very flat $\frac{7}{2}^-$.
$Pb^{208}(p,d)Pb^{207}$	$3p$	28.0	Differences between $\frac{1}{2}^-$ and $\frac{3}{2}^-$ curves are hardly noticeable.
$Pb^{208}(p,d)Pb^{207}$	$2f$	28.0	Little, if any, J dependence.
$Fe^{56}(He^3,\alpha)Fe^{55}$	$1f$	30,40	Small phase difference between $\frac{5}{2}^-$ and $\frac{7}{2}^-$ distributions.

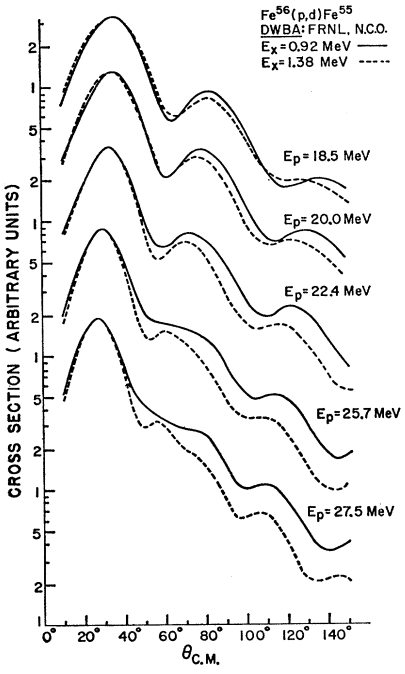

FIG. 23. DWBA calculations for $l=3$ transitions in $Fe^{56}(p,d)Fe^{55}$ with a spin-orbit potential strength of 8.0 MeV included in both the proton and deuteron optical potentials.

compared be approximately equal. Although the shapes of the $l=1$ distributions change more rapidly with energy than $l=3$ curves, each $\frac{1}{2}^-$ curve retains a distinctive character that is quite different from all the $\frac{3}{2}^-$ curves. On the other hand, a high-energy $\frac{7}{2}^-$ angular distribution is similar to a lower energy $\frac{5}{2}^-$ curve.

The DWBA was not successful in explaining this J dependence. A short summary of the various calculations described in Sec. IV is included in Table IV. These results indicate that a spin-orbit potential, which could account for J dependence in the (p,α) reaction, has only a small influence on both $l=1$ and $l=3$ (p,d) predictions. The significant features of the $\frac{1}{2}^-$ curves could not be explained well at any energy; the DWBA matched the more gentle diffraction pattern of the $\frac{3}{2}^-$ rather than the sudden dips or the pronounced maxima and minima of the $\frac{1}{2}^-$. The forward-angle region of $l=3$ curves was not affected by the spin-orbit forces at low energies; at higher energies, the effect was in the wrong direction.

Our analysis by no means exhausted the possible optical parameters that might be used in JULIE. We generally used potentials that could be found in the literature, and did not attempt to reanalyze the elastic scattering data from which they were derived. Some runs were made with one or two of the parameters in a particular set changed by as much as 50%, but clearly this could not be done with all the potentials. Since the predicted J dependence changed so little when the various sets of optical parameters available were used, however, there are no indications from our work that the solution to the problem lies in obtaining different or more exact parameters for the type of optical potential used here. This does not eliminate from consideration complex spin-orbit terms, or spin-orbit potentials with

TABLE IV. Summary of DWBA calculations for $Fe^{56}(p,d)Fe^{55}$.

Type of calculation	Results
	(A) $l=1$
Standard	With CO at 4.75 F, fit to $\frac{3}{2}^-$ data is good, especially at higher energies. Predicted $\frac{1}{2}^-$ curves are very similar to $\frac{3}{2}^-$; since data show large J dependence, this implies that fit to $\frac{1}{2}$ is not good. NCO predictions have too little structure; even in FRNL calculation, CO curves are better.
L·S	Addition of spin-orbit coupling to proton and deuteron optical potential had little effect on either $\frac{3}{2}^-$ or $\frac{1}{2}^-$ distributions, and seldom gave any hint of predicting J dependence of data. At low energies, fit to 70° J dependence is worse when **L·S** coupling is added; fit to back angles is probably slightly better. At high energy, DWBA predicted only small phase change between $\frac{1}{2}^-$ and $\frac{3}{2}^-$ at large angles.
Form factor adjustment	Use of effective binding of 8.0 MeV for $\frac{3}{2}^-$ and 6.0 MeV for $\frac{1}{2}^-$ neutron did not produce any J dependence, though it did slightly improve quality of fits by shifting predicted distributions more forward.
	(B) $l=3$
Standard	NCO predictions fit data better than CO. At high energy, NCO fits $\frac{7}{2}$ rather well; $\frac{5}{2}$ prediction similar to $\frac{7}{2}$ so that the $\frac{5}{2}$ fit is poor over forward maximum. At lower energies NCO, like CO, falls off too much at large angles; forward angle prediction midway between $\frac{5}{2}$ and $\frac{7}{2}$ data. In FRNL, NCO curves for $\frac{5}{2}$ and $\frac{7}{2}$ drop off more rapidly from forward maximum than LZR curves; thus, $\frac{5}{2}$ fit improves, $\frac{7}{2}$ fit deteriorates. Neither fits well. FRNL, CO curve has about the same shape as LZR, CO curve.
L·S	Including spin-orbit coupling in proton and deuteron channel has small effect, which usually makes fit to J dependence worse.
Effective binding versus separation energy form factor	At high energies, LZR, NCO predictions with EB form factors fit both $\frac{5}{2}$ and $\frac{7}{2}$ data rather well over forward maximum; $\frac{5}{2}$ prediction is too low at back angles. At lower energies, predicted forward angle J dependence is somewhat smaller and matches neither $\frac{5}{2}$ nor $\frac{7}{2}$. EB distributions were not affected by FRNL corrections as SE distributions were; consequently, FRNL calculations do not fit data at any energy.
Variable radius of form factor	Increasing radius of $\frac{5}{2}$ neutron potential well to 5.7 F and decreasing $\frac{7}{2}$ well radius to 4.0 F are even less effective than using EB form factors. At lowest energies, predicted J dependence is in fact opposite of that experimentally observed.
Combined form factors	Joining SE tail to EB interior wave function showed that essentially all difference between SE and EB predictions originates in region where the radius is larger than 5 F; significant differences arise even from radii larger than 7 F.

shapes radically different from the Thomas form used here.

Simple variations in the form factor were also shown to be ineffective in producing J dependence. We have noted that the introduction of finite range and nonlocal potentials greatly decreased the difference between the distributions calculated with the two prescriptions; it was also found that much of the difference could be eliminated if the correct asymptotic tail was joined to the EB form factor at a radius of 6 or 7 F. Further, even the LZR predictions with an effective binding indicated that the J dependence should decrease significantly at lower energies, while the data show a J dependence which is just as pronounced at 18.5 MeV as it is at 27.5 MeV. The change in the radius of the potential well seen by $\frac{5}{2}^-$ and $\frac{7}{2}^-$ neutrons was even less successful in predicting the observed differences.

The failure of the DWBA to fit the observed distributions with these modified form factors is of spectroscopic interest. The absolute magnitudes of the cross sections predicted with the various form factors can differ by factors of two or three, so that the spectroscopic factors derived from the data also differ by the same factors. The fits to the 27.5-MeV J dependence previously found[2] have usually been cited as some justification for choosing an effective binding energy. The present results show that these good fits were somewhat fortuitous, and that the quality of the fits to all the data does not significantly change when the form factor is altered in the manner described. Thus, this work gives no evidence that, in the absence of more realistic wave functions and form factors, the normal separation energy prescription should not be followed when extracting spectroscopic factors.

The fact that adjustments to the form factor are not of much help in accounting for J dependence means that other explanations must be sought, and it is not clear that these consist in more drastic modifications of the neutron well. Since the work of Pinkston and Satchler[37] and Austern[36] showed that the effective well seen by a particle depends critically on the configurations making up the state, it would be expected that a J dependence attributable to such modifications would change considerably from nucleus to nucleus. A detailed study of the variations with mass number of J dependence has yet to be reported, but the evidence indicates that there is little change. Our $Ni^{58}(p,d)$ distributions agree well with the $Fe^{56}(p,d)$ results, and the data of Whitten[29] on the Cr isotopes at 17.5 MeV also corroborate the Fe data. Certainly, the gross features of forward angle J dependence are well reproduced from one nucleus to another in the targets studied by Sherr *et al.*[2] Since the forward-angle J dependence for $1d$ transfer is so similar to that seen with $l=3$, it seems likely that both arise from the same mechanism. But here again there are no large variations with nuclear structure; the same sort of spin-dependent distributions are seen in reactions on O^{16}, Mg^{24}, Si^{28}, S^{32}, and Ca^{40}.

This reasoning also argues against a solution based on strong inelastic scattering in either the entrance or exit channel. The strength of the inelastic scattering would be expected to vary markedly from isotope to isotope, certainly e.g., from Mg^{24} to Ca^{40}. Since the observed J dependence is much the same for all these nuclei, it does not seem that second- or higher-order corrections to the distorted waves will give a consistent explanation.

ACKNOWLEDGMENTS

We are indebted to Professor R. Sherr for his continuing interest and support, and for many hours of critical discussion. We gratefully acknowledge the advice of Dr. E. Rost on DWBA calculations, and also helpful discussions with Dr. R. H. Bassel and G. R. Satchler. Our thanks are due to Dr. Michaya Kondo and R. G. Matlock for their experimental help, and to Leonard Fellman and Stuart Feldman for their aid with the calculations. We are grateful also to Dr. R. H. Bassel, J. K. Dickens, and R. Drisko for making their computer programs available to us. One of us (C.G.) deeply appreciates the generous hospitality of the entire staff at the University of Colorado Nuclear Physics Laboratory during a lengthy stay; I want to thank particularly Professor D. Lind and Professor J. Kraushaar. The technical competence of the entire crew there is admired and appreciated. Many calculations were carried out on the Princeton computer facilities, which are supported in part by the National Science Foundation under Grant No. NSF-GP 579.